ISSN 0006-3509, Biophysics, 2018, Vol. 63, No. 2, pp. 248–253. © Pleiades Publishing, Inc., 2018.
Original Russian Text © A.V. Zherebtsov, N.S. Tropskaya, 2018, published in Biofizika, 2018, Vol. 63, No. 2, pp. 342–348.

COMPLEX SYSTEMS BIOPHYSICS

Application of the Gabor Transform for Analysis of Electromyographic Signals of the Intestine in the Low-Frequency Region

A. V. Zherebtsov[a], * and N. S. Tropskaya[a]
[a]*Sklifosovsky Research Institute of Emergency Medicine, Moscow Department of Health, Moscow, 129090 Russia*
**e-mail: alexey1235@mail.ru*
Received November 8, 2017

Abstract—The Gabor transform allows quantitative estimation of the non-stationarity of the electromyographic signal in the low-frequency region with the maxim permissible time–frequency resolution. The calculation of the parameters of the Gabor transform was conducted on different time and frequency intervals to estimate the slow-wave activity of the intestine. It was demonstrated that the efficient size of the 32-s time window, which provides the efficient resolution of the frequency spectrum at 0.01 Hz, is suitable for the accurate study of the change in the frequency of slow waves. The ability to construct the dependence of the change in the frequency of slow waves of electromyograms on time with the specified accuracy was demonstrated.

Keywords: Gabor transform, intestine electromyogram, slow waves
DOI: 10.1134/S0006350918020276

INTRODUCTION

Slow-wave activity associated with membrane-potential fluctuations is peculiar to the smooth muscles of the intestine. Slow waves are not directly related to contractions, but are a factor in synchronizing and coordinating contractions [1]. The literature data also show that there is a proximal–distal gradient of the frequencies of slow waves throughout the intestine. Thus, for example, the frequency of slow waves of the small intestine in rats changes in the proximal–distal direction from 0.7 to 0.4 Hz [2, 3].

The slow-wave frequency varies in a narrow range with long-term registration of an electric signal in a particular region of the smooth-muscle tissue of the intestine; this can be explained by many factors, including electric potential input from neighboring tissue regions. Thus, the electromyographic signal of the small intestine is not stationary in time.

The inability to provide both good time and frequency resolution simultaneously is the main difficulty during time–frequency analysis of these signals (the narrower the signal time region is, the higher the time resolution is and the lower the frequency resolution is).

The window Fourier transform (WFT), Gabor transform (the WFT with a Gaussian function as a window), continuous wavelet transform, and Hilbert transform are used for the time–frequency analysis of bioelectric signals [4]. The Gabor transform is characterized by the maximum resolution in the time–frequency region and by a fixed size of the sliding time window for all of a studied frequency range. The use of the Gabor transform is appropriate in the case of a change in the studied signal frequency in a relatively small region. Thus, by choosing the length of the sliding window, it is possible to obtain the optimal frequency resolution fixed at all of the studied frequency range.

The aim of this work was to justify the application and to select the parameters for the Gabor transform in the analysis of slow-wave activity in the intestine.

MATERIALS AND METHODS

Analysis of the electromyograms of the small intestine with a duration of 3600 s obtained in chronic experiments on rats in the Laboratory of Experimental Pathology of the Sklifosovsky Research Institute of Emergency Medicine was conducted in this work.

The basic scheme of the implantation of electrodes was as follows: monopolar needle electrodes were implanted during the preliminary operational training in the serous–muscular layer of the small intestine wall in rats and their wires were led out through the tail; the reference comparison electrode was anchored in the internal part of the abdominal wall and was also led out through the tail. Thus, a monopolar scheme of electromyographic signal registration was used. An NVX-52 electron encephalograph (OOO MKS, St. Petersburg) was used as a bioelectric signal amplifier. The signal recording was conducted in the frequency

Abbreviations: WFT, window Fourier transform.

band from 0.05 to 35 Hz at the discretization frequency of 250 Hz.

In order to accurately estimate changes of the slow waves in the frequency region, a particular case of WFT (namely, the Gabor transform) was selected. The best uncertainty ratio in the time–frequency region, as well as the constant time-window size (and, as a consequence, a fixed resolution in the frequency region), were the main criteria in the selection of this approach; this provided good conditions for quantitative study of the changes in the slow-wave frequency fluctuation in a relatively narrow range.

The calculations were carried out using the functions of the Python 3.6 programming language. In particular, the NumPy and SciPy libraries were used to construct the signal-processing algorithms; The Matplotlib library was used for visualization of the data.

RESULTS

The discrete signal Gabor transform. In general, for a function $f(t) \in \mathbb{L}^2(\mathbb{R})$, the WFT has the form:

$$F(\omega, \tau) = \int_{-\infty}^{\infty} f(t)\gamma(t-\tau)e^{-i\omega t}dt, \quad (1)$$

where $\gamma(t)$ is a window function that decreases rapidly at infinity and $\gamma(t) \in \mathbb{L}^2(\mathbb{R})$, $t\gamma(t) \in \mathbb{L}^2(\mathbb{R})$, and $\tau \in \mathbb{R}$, are the size of the shift of the window function. Here, $F(\omega, \tau_w)$ is called the signal spectrum $f(t)$, which is obtained as a result of the WFT depending on the window-function shift (τ_w). The window-function spectrum has the form

$$\Gamma(\omega) = \int_{-\infty}^{\infty} \gamma(t)e^{-i\omega t}dt. \quad (2)$$

The radius of the window function and the radius of the window-function spectrum are the characteristics of the window function. The window-function radius is determined as

$$\Delta_t = \frac{\left(\int_{-\infty}^{\infty}(t-\overline{t})^2\gamma^2(t)dt\right)^{\frac{1}{2}}}{\left(\int_{-\infty}^{\infty}\gamma^2(t)dt\right)^{\frac{1}{2}}}, \quad (3)$$

where $\overline{t} = \dfrac{\int_{-\infty}^{\infty} t\gamma^2(t)dt}{\int_{-\infty}^{\infty}\gamma^2(t)dt}$.

Accordingly, the radius of the window-function spectrum is determined as

$$\Delta_\omega = \frac{\left(\int_{-\infty}^{\infty}(\omega-\overline{\omega})^2\Gamma^2(\omega)d\omega\right)^{\frac{1}{2}}}{\left(\int_{-\infty}^{\infty}\Gamma^2(\omega)d\omega\right)^{\frac{1}{2}}}, \quad (4)$$

where $\overline{\omega} = \dfrac{\int_{-\infty}^{\infty}\omega\Gamma^2(\omega)dt}{\int_{-\infty}^{\infty}\Gamma^2(\omega)dt}$.

The values $\overline{t}$ and $\overline{\omega}$ are called the window-function centers. The multiplication of two radii satisfies the following inequality:

$$\Delta_t\Delta_\omega \geq \frac{1}{2}. \quad (5)$$

This equation only occurs for the Gaussian window function

$$\gamma_\alpha(t) = \frac{1}{2\sqrt{\pi\alpha}}e^{-\frac{t^2}{4\alpha}}, \quad (6)$$

where $\alpha \in \mathbb{R}$, $\alpha > 0$.

The inequality (5) indicates that it is impossible to determine t and ω accurately at the same time, but only with some degree of uncertainty [5]. Thus, using the Gaussian function as a window in the Fourier transform, we obtain the best ratio of the time–frequency resolution. The WFT with a Gaussian function as a window is called the Gabor transform. Based on the expressions (3), (4), and (6) it is possible to calculate that $\Delta_t = \sqrt{\alpha}$ and $\Delta_\omega = \frac{1}{2\sqrt{\alpha}}$ for the Gabor transform [6].

A discrete signal with the specified discretization frequency Δt_{disc} and final number of counts $N \in \mathbb{N}$ is considered. The signal is then divided into the sample of values $t_n = n\Delta t_{\text{disc}}$ for $n = 0, 1, 2 \ldots N-1$ and it is possible to make a transition to a discrete window Gabor transformation:

$$F(\omega_k, \tau_l) = \Sigma_{n=0}^{N-1} f(n\Delta t)\gamma_\alpha(n\Delta t - \tau_l)e^{-i\omega_k n\Delta t}, \quad (7)$$

where $\omega_k = \frac{2\pi k}{N\Delta t}$, $\tau_l = l\Delta t$, $k = 0, 1, 2, 3 \ldots N-1$, $l = 0, 1, 2 \ldots N-1$. Thus, we obtain:

$$F(k, l) = \Sigma_{n=0}^{N-1} f(n\Delta t)\gamma_\alpha((n-l)\Delta t)e^{-i\frac{2\pi k}{N}n}. \quad (8)$$

Formula (8) allows one to carry out the Gabor transform of the discrete signal for different window-function shifts and to construct the dependence of local discrete Gabor spectra on time. The efficient spectral resolution is determined as $d_\omega = 2\Delta_\omega$; the efficient time window width $d_t = 2\Delta_t$. Thus, we obtain from expression (5) and the calculated values for Δ_t and Δ_ω:

$$d_t d_\omega = 2,\quad \alpha = \frac{d_t^2}{4},\quad \alpha = \frac{1}{d_\omega^2}. \tag{9}$$

It is more convenient to work with linear frequencies expressed in hertz during the analysis of electromyograms. It is possible to transform the expressions in (9) to the appropriate form setting $d_\omega = 2\pi d_\nu$, where d_ν is the efficient spectral resolution expressed in hertz:

$$d_t d_\nu = \frac{1}{\pi},\quad \alpha = \frac{d_t^2}{4},\quad \alpha = \frac{1}{4\pi^2 d_\nu^2}. \tag{10}$$

Separately, it is worth noting that the efficient spectral resolution d_ω differs from the spectrum discretization frequency and contains information about the accuracy of the frequency determination on a specified efficient time-window size. The spectrum discretization frequency from expression (7) is

$$\Delta\nu = \frac{1}{N\Delta t}.$$

In the general case, the Gabor transform spectrum is a complex function that contains information about the phase and amplitude of the appropriate frequency component. When constructing spectra in this work, we take the value $|F(\omega,\tau)|$, which only carries information about the amplitude.

The Gabor transform during calculation of the spectrum of electromyograms. The Kotelnikov theorem, which states that any function $F(t)$ that consists of frequencies from 0 to ν_0 can be continuously transmitted using numbers that follow each other in $\Delta t = \frac{1}{2\nu_0}$ seconds, is used. Thus, assuming that the frequencies of the slow-wave activity of the rat small intestine are in the range from 0 to 1 Hz, it is possible to decrease the discretization interval of an initial signal to 0.5 s per one count. The fast Fourier transform algorithm is used everywhere below to construct the Gabor transform frequency spectra. The performance of the fast Fourier transform algorithm restricts the number of analyzed signal counts and assumes that their amount is equal to the degree of the number two, that is, $N = 2^n$, $n \in \mathbb{N}$. With the signal duration of 3600 s and signal discretization interval $\Delta t = 0.5$ s, we obtain the nearest number $N = 8192$. Thus, by lowering the discretization interval of the initial electromyogram and filling the missing number of counts with zeros, we obtain the discretization frequency of the spectrum obtained during the fast Fourier transform from expression (11): $\Delta\nu = \frac{1}{8192 \cdot 0.5c} \cong 10^{-4}$ Hz. It should be noted that the signal addition with zeros changes the discretization frequency of the spectrum of the entire signal according to the expression (11) [7]. The parameter α, which

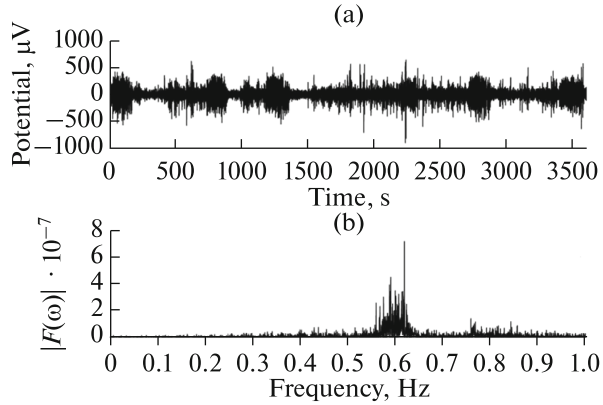

Fig. 1. An electromyogram of the proximal part of the jejunum with a duration of 3600 s (a), the frequency spectrum in the slow-wave region from 0 to 1 Hz (b).

is required to perform the Gabor transform and to construct the frequency spectrum of the entire signal, is calculated from expression (10). The efficient time-window width in this case will be $d_t = 3600$ s, the efficient spectral resolution $d_\nu \cong 10^{-4}$ Hz, and the parameter $\alpha = 3.24 \cdot 10^6$ s^2. An example of the frequency spectrum of the entire electromyogram is presented in Fig. 1.

It is seen from Fig. 1 that the frequency of slow-wave activity is in the range $\Delta\upsilon_{SW} \cong 0.1$ Hz throughout all of the electromyogram and reaches a maximum at the frequency $\upsilon_{SW} \cong 0.6$ Hz. The common amplitude–frequency characteristics of the slow-wave activity for the considered region of the intestine can be found from the amplitude spectrum of the Gabor transform with a continuous window width. To track changes in the slow-wave activity depending on time, it is necessary to have amplitude–frequency information from electromyogram regions of a small duration. To analyze the amplitude–frequency distribution of slow waves in certain electromyogram regions it is necessary to decrease the value of the efficient time-window width in the Gabor transform, due to which a decrease in the efficient spectral resolution will occur in the frequency region d_ν. From expression (10), it is possible to find the efficient time window width for different resolutions in the frequency region or the resolution in the frequency region for different efficient time-window widths. The calculated parameters α and d_t for $d_\nu = 0.1$, 0.01, and 0.001 Hz, respectively, are given in Table 1.

The electromyographic signal spectrum presented in Fig. 1 shows the expediency of the study of frequency behavior at different regions of smaller durations with the frequency resolution in $d_\nu \cong 0.01$ Hz. Thus, we obtain a high level of time localization with $d_t \cong 32$ s. As stated above, a further decrease in the window width decreases the resolution in the fre-

Table 1. The parameters of the Gabor transform for different efficient spectral resolutions

Resolution by d_ν frequency, Hz	α coefficient, s^2	Efficient window width d_t, s
0.1	2.53	3.2
0.01	253	32
0.001	25330	320

quency region and it will be impossible to obtain any new information from the spectrum at $d_t \cong 3.2$ s with the resolution $d_\nu \cong 0.1$ Hz. Different electromyogram regions with a duration of 32 s and their spectra with the appropriate efficient resolution in the 0.01 Hz frequency region are given in Fig. 2.

It can be seen from Table 2 that the amplitude maximum is reached at different frequencies for different time regions of the electromyogram given in Fig. 2. The clearly pronounced amplitude peak on all of the given spectra allows us to uniquely identify the slow-wave frequencies in the considered time periods.

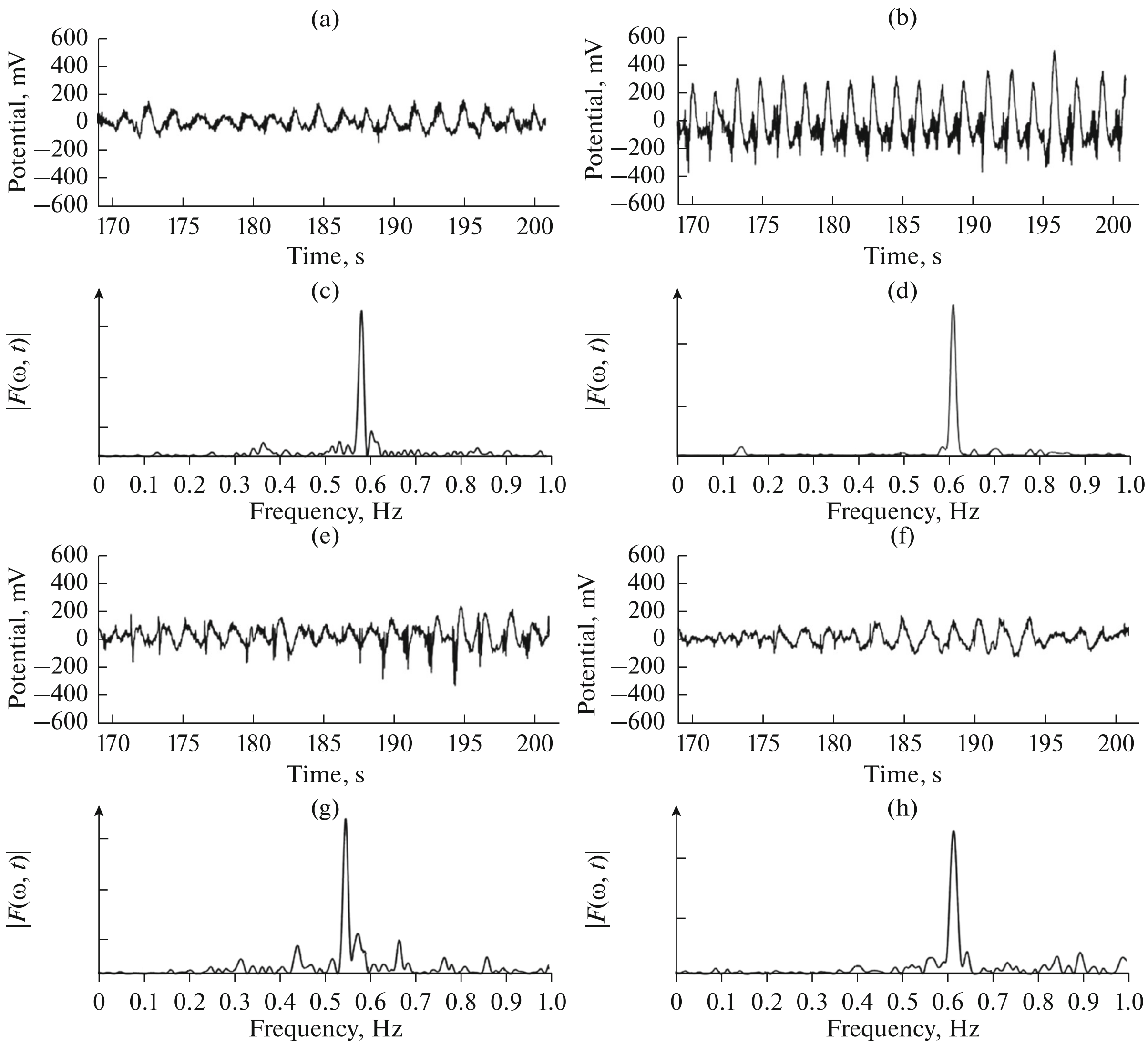

Fig. 2. Time regions of an electromyogram and their spectra with centers of time-window functions $\bar{t} = 185$ s (a, c), $\bar{t} = 1220$ s (b, d), $\bar{t} = 2670$ s (e, g), $\bar{t} = 3185$ s (f, h) and the efficient window size of the Gabor transform $d_t = 32$ s.

Table 2. Spectral estimation of the slow-wave frequency with an efficient spectral resolution of 0.01 Hz for different values of window-function centers with an efficient width of 32 s

Window-function center, $\bar{t}$, s	Efficient window width, d_t, s	Slow-wave frequency υ_{SW}, Hz
185	32	0.59
1220	32	0.62
2670	32	0.62
3185	32	0.55

The ability to analyze the dynamics of changes in the slow-wave frequency over time. The Gabor transform on a sliding time window is applied to construct a picture of the changes in the slow-wave frequency over time. The efficient width of the time window is 32 s, the time step is accepted as 1 s. The frequency on the spectrum that corresponds to the amplitude maximum will be taken as the slow-wave frequency on the instantaneous spectra of the sliding time window. The initial electromyogram is given in Fig. 3a; the dependence of the frequency on time that is thus constructed is shown in Fig. 3b. The fact should be taken into account that the time-frequency localization obeys the uncertainty ratio (5). Each time moment on the frequency–time graph corresponds to the time of the time window shift τ, and it is possible to talk only about the presence of certain frequency in the time region, which corresponds to the efficient time window width and this shift.

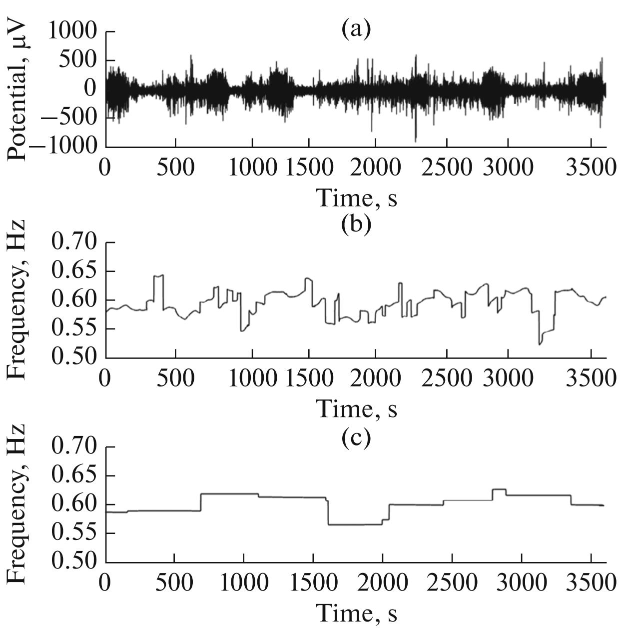

Fig. 3. An electromyogram of the proximal part of the jejunum with a duration of 3600 s (a), the dependence of the slow-wave frequency on time for d_t = 32 s (b) and d_t = 320 s (c).

The Gabor transform on a sliding time window with an efficient width that differs on the larger side, that is, 320 s, is applied to the signal. The thus-obtained frequency–time dependence reflected in Fig. 3c demonstrates the more stable behavior of the slow-wave frequency throughout the entire signal. At the same time, the lack of stability of the slow-wave frequency depending on time is clearly observed and preserved. It is seen from Fig. 3 that an increase in the time-window size decreases the effect of local and short-term (relative to the window size) signal amplitude jumps on the frequency spectrum. Such components are often a reason for the false identification of the slow-wave frequency under conditions of artifact signal noise or the presence of another process that is not related to slow waves that has a complex frequency–time structure.

CONCLUSIONS

The application of the Gabor transform and construction of spectra of different electromyogram regions allows one to identify the slow-wave frequency with the maximum frequency–time localization. The presence of a clear single amplitude peak in the slow-wave frequency range is typical after the application of the Gabor transform on all spectra of the analyzed electromyogram regions. It was demonstrated that the maximum amplitude peaks on the spectrum can correspond to different frequencies that depend on time. Thus, the frequency range of the slow-wave activity of the studied region of the intestine observed on electromyogram spectra of a large duration (3600 s) is explained by a change in the slow-wave frequency over time. Consequently, the Gabor transform allows one to establish the presence and to study the non-stationarity of an electromyographic signal in the slow-wave activity region with sufficient accuracy (0.01 Hz) and the maximum possible time localization (32 s) for this resolution.

REFERENCES

1. R. Lees-Green, P. Du, G. O'Grady, et al., Front. Physiol. **2**, 29 (2011).
2. C. L. Prosser and A. Bortoff, in *Handbook of Physiology,* 2nd ed. (Williams & Wilkins, Baltimore,1968), **Vol. 4**, pp. 2025–2050.
3. M. Ruckebusch and J. Froramonti, Gastroenterology **68** (6), 1500 (1975)
4. M. Wacker and H. Witte, Methods Inf. Med. **52**, 279 (2013)
5. M. N. Yudin, Yu. A. Farkov, and D. M. Filatov, *An Introduction to Wavelet Analysis* (Moscow, 2001) [in Russian].
6. I. Ya. Novikov and S. B. Stechkin, Usp. Matemat. Nauk **53** (6), 53(1998).
7. N. I. Seregin, *Specific Features of Using Discrete Fourier Transform in Spectral Analysis* (Yekaterinburg, 2006) [in Russian]. http://www.study.urfu.ru/Aid/Publication/388/1/seregin.pdf.

Translated by A. Barkhash